Nano Research 2013, 6(6): 389–398
DOI 10.1007/s12274-013-0316-8
Research Article
ISSN 1998-0124
CN 11-5974/O4

Design of multi-functional dual hole patterned carbon nanotube composites with superhydrophobicity and durability

Sung-Hoon Park[1,§] (✉), Eun-Hyoung Cho[1,§] (✉), Jinseung Sohn[1], Paul Theilmann[2], Kunmo Chu[1], Sunghee Lee[1], Yoonchul Sohn[1], Dongouk Kim[1], and Byunghoon Kim[1]

[1] *Samsung Advanced Institute of Technology, Yong-in, 446-712, R. O. Korea*
[2] *Department of Electrical Engineering, University of California, San Diego, La Jolla, California 92093, USA*
[§] *These authors contributed equally to this work*

Received: 24 February 2013
Revised: 31 March 2013
Accepted: 6 April 2013

KEYWORDS
dual hole,
nanoimprint lithography,
superhydrophobic,
arbon nanotube,
durability,
multifunction

ABSTRACT

Most current research on nanocomposites has focused on their bulk attributes, i.e., electrical, microwave, thermal, and mechanical properties. In practical applications, surface properties such as robustness against environmental contamination are critical design considerations if intrinsic properties are to be maintained. The aim of this research is to combine the bulk properties of nanocomposites with the superhydrophobic surface properties provided by imprinting techniques to create a single multi-functional system with enhanced bulk properties. We report the development of a highly conductive superhydrophobic nanotube composite, which is directly superimposed with a durable dual hole pattern through imprinting techniques. The dual hole pattern avoids the use of high slenderness ratio structures resulting in a surface which is robust against physical damage. Its stable superhydrophobic properties were characterized both theoretically and experimentally. By incorporating high aspect ratio carbon nanotubes (CNTs), the dual patterned composites can also be effectively used for anti-icing and deicing applications where their superhydrophobic surface suppresses ice formation and their quick electric heating response at low voltage eliminates remaining frost. In addition, superior electromagnetic interference (EMI) shielding effectiveness (SE) was attained, with one of the highest values ever reported in the literature.

1 Introduction

Polymer composites containing conducting fillers have been extensively investigated for various applications such as electromagnetic interference (EMI) shielding, electronic packaging, radar absorption, structural reinforcement, high charge storage capacitors and heating units [1–4]. High aspect ratio fillers which

Address correspondence to Sunghoon Park, leo.park@samsung.com; Eunhyoung Cho, cchoeh@samsung.com

attain electrical percolation at low volume fractions are exceedingly desirable due to the structural integrity and electronic properties of the resulting composites. Carbon nanotubes (CNTs) offer an attractive option in this regard; they exhibit an extremely high aspect ratio which can reach up to 10^6. This coupled with a large interfacial area (> 1,300 m^2/g), allows composites which use CNT fillers to have mechanical and microwave properties that far exceed those of the initial polymer matrix [5–8]. However, most current research on nanocomposites has focused on their bulk attributes, i.e., electrical, microwave, thermal, and mechanical properties. In practical applications, surface properties such as robustness against environmental contamination are critical design considerations if intrinsic properties are to be maintained. For example, in anti-icing (the preventing of frost formation) applications, superhydrophobic coatings have been shown to effectively suppress ice formation in situations where uncoated surfaces fail [9]. In addition, the performance of a microwave absorbing material—which is sensitive to its thickness—could be modified through an unwanted contamination layer [10].

Superhydrophobic surfaces with a water contact angle (WCA) above 150° and water sliding angle lower than 5° have attracted extensive research interest in both the scientific and engineering fields [11, 12]. Due to their potential convenience, superhydrophobic surfaces and materials have been investigated for various applications such as anti-snow sticking, blood compatibility, self-cleaning, and micro-fluidic systems [13–16]. In general, superhydrophobic surfaces are created by coating samples with low-surface-energy materials and/or controlling surface roughness through the design of structures at both the micro- and nanoscale [17]. Approaches to achieving such conditions include chemical etching, the use of nanotube arrays and solvent casting, the latter possibly being the method most amenable to practical applications [18–20]. With a proper solvent and temperature selection, solvent casting can be used to form polypropylene (PP) into a porous gel coating which has a WCA of 160° [11]. Furthermore, in conjunction with conjugated conducting polymers, solvent casting can be used to create conducting, superhydrophobic coatings which can be applied to various substrates [21]. However, such methods are not applicable to all applications due to the requirements put on the underlying base structure/substrate to ensure adhesion. In addition, durability and uniformity issues are still in need of improvement. In other approaches, a soft lithographic imprinting method has been developed to fabricate superhydrophobic surfaces. For example using a polydimethylsiloxane (PDMS) stamp, which was prepared by replica molding against a hydrophobic lotus leaf surface, a mimicked surface was transferred to a substrate through imprinting [22]. In such a process, the highest WCA is achieved when a complicated pattern or a pattern having a high slenderness ratio is used. Unfortunately, these patterns are easily damaged by physical contact, thereby reducing their potential use in practical applications.

The aim of this research is to combine the bulk properties of nanocomposites with the superhydrophobic surface properties provided by imprinting techniques to create a single multi-functional system with enhanced bulk properties. We report the development of a highly conductive superhydrophobic nanotube composite, which is directly superimposed with a durable dual hole pattern through imprinting techniques. The dual hole pattern was designed to avoid the use of high slenderness ratio structures resulting in a surface which is robust against physical damage.

2 Experimental

2.1 Sample preparation

For the fabrication of nanocomposites, polydimethylsiloxane (PDMS: Sylgard 184 SILICONE ELASTOMER BASE) was purchased from Dow Corning, and multiwalled carbon nanotubes (MWCNTs) having 10–20 nm outer diameter and 100–200 μm length were purchased from Hanwa Nanotech Inc. To ensure effective mixing and dispersion of the highly entangled CNTs within the polymer matrix, premixing (Paste mixer, Dae Hwa Tech, PDM-1k) and a three-roll milling technique (Ceramic 3 roll mill, INOUE MFG., INC) were used. Briefly, MWCNTs of varying weight percentages and the PDMS base elastomer were combined using the following procedure. First the elastomer base and curing agent were mixed in a ratio of 10:1,

w/*w*. This material was then mixed with the CNTs in the paste mixer for 1 min to form a CNT paste. Then, the CNT pastes were three-roll milled for several minutes while gradually decreasing the gap between the rolls. Conventional photolithography and electroplating processes were utilized to prepare a nickel stamp for superhydrophobic dual hole patterning of the CNT composites. The thermal imprinting was processed using an in-house system. After loading the nickel stamp onto the CNT pastes, optimal imprinting parameters, including a vacuum pressure of 0.4 Torr, pressing force of 240 kgf, delay time of 270 s, and curing time of 30 min at 120 ˚C, were established for high-fidelity patterning. Subsequently, the nickel stamp was carefully peeled off the cured CNT composites after they had completely cooled, leaving a dual hole pattern on the CNT composite surface.

2.2 Characterization

Morphology and structural features of the dual hole patterned CNT composites were characterized using an optical microscope (Olympus) and scanning electron microscopy (SEM: Hitachi, field emission SEM, S-4500 XL30 and Quanta, field emission SEM, 650 FEG). The WCA and contact angle hysteresis (CAH) were acquired using a contact angle measuring instrument (DSA 10 Mk2, Krüss) with a drop shape analysis system. The volume of the deionized (DI) water droplets was around 7 μL. The average WCA was obtained at a minimum of at least five different places to ensure measurement accuracy. The CAH was measured just before rolling off when the sample on the stage was tilted. To investigate wear durability of patterned composites films, a wear tester was constructed. Briefly, rubber-tipped glass having a radius of 2.5 mm under applied normal loads of 1.5 N was moved horizontally with a sliding speed of 25 mm/s. After the wear test, the WCA and SEM images were used to characterize any change in surface properties.

To evaluate the electrical heating behavior of the superhydrophobic patterned CNT composites, a direct electric current was applied to the sample using a National Instruments, NI PXI-1033 chassis. Then, thermal infrared images were recorded with a thermal infrared camera (Advanced Thermo, TVS-500). The dual hole patterned CNT/PDMS composites were cut into a rectangular shape of 20 × 40 mm^2, with a thickness of around 500 μm. The heater was composed of two layers, polyimide (PI) film/CNT composite and a copper conductor which acted as an electrode. To ensure electrical contact, a conductive silver paste was used between the samples and copper conductors. The electromagnetic properties of the dual hole pattern CNT composites, as measured through the S-parameters (S_{ij}), were recorded in the microwave frequency range (8.2–12.4 GHz, X-band) using a vector network analyzer (Agilent 5242A PNA-X). The CNT/PDMS paste was heat pressed with a dual patterned master stamp into a 2 mm thick sample holder of size 0.9" × 0.4"—a standard WR-90 waveguide size suitable for the X-band frequency range. Then, the composite-loaded holder was inserted between two 15 cm lengths of WR-90 X-band waveguide to mitigate the near-field effects of the coax to waveguide transitions.

3 Results and discussion

3.1 Design of dual hole pattern

A superhydrophobic surface with an extremely high contact angle and low hysteresis can be achieved by creating hierarchical roughness on low surface energy materials. The maximum contact angle is obtained by packing the asperities as tightly as possible. The dual hole hexagonal distribution designed and used in this work results in a very high asperity density. Moreover, liquids in the Cassie state generally exhibit lower slide angles and contact angle hysteresis than those in the Wenzel state [23]. According to the Cassie model, air is trapped below the liquid droplet, forming "air pockets". Thus, hydrophobicity is increased as the drop sits partially on air. Using Young's equation, a contact angle of θ^* can be obtained [24]

$$\cos\theta^* = \varphi_s(\cos\theta_0 + 1) - 1 \quad (1)$$

where φ_s is the fraction of the solid/liquid interface below the droplet and θ_0 is the static contact angle for the given surface tension. For a hexagonal closely packed circular hole surface, the fraction of the solid/liquid interface φ_s is given by

$$\varphi_s = 1 - (\pi/2\sqrt{3})\cdot\lambda^2 \quad (2)$$

where λ is the ratio of the hole radius to the maximum hole radius. The surface roughness r has a considerable influence on both the contact angle itself and its hysteresis. Since it can be defined as the ratio of the real surface area to the apparent surface area, r of a given geometry is expressed by

$$r = 1 + \sqrt{6} \cdot \pi \cdot \lambda \cdot h / 3p \quad (3)$$

where h is the hole depth and p is the pattern pitch. If the contact angle θ is between 90° and θ_c given by $\cos\theta_c = (\varphi_s - 1)/(r - \varphi_s)$, the regime is considered metastable (Wenzel state). For angles θ larger than θ_c, the regime is said to be stable (Cassie state). Based on these theories, a dual hole pattern which consists of arrays of small and large-sized hexagonal holes was designed. The hexagonal pattern design (small and large) is detailed in Fig. 1(e) where d indicates the hole diameter and p specifies the hole-to-hole pitch.

Design parameters as well as theoretical and experimental WCAs for hexagonal closely packed circular hole surfaces are summarized in Table 1. The measured static WCA of the raw polymer materials without patterning for hydrophobicity is approximately 110°. The small hole array by itself exhibits a calculated critical WCA θ_c that is smaller than 110°. Thus, while the small hole patterned material is stable, the WCA is too low for it to be considered superhydrophobic. On the other hand, the large hole array patterned material is superhydrophobic but also metastable due to its large WCA (θ_c > 110°). The dual hole pattern combines the desired stability of the small hole array with the superhydrophobic properties of the large hole array. Its initial WCA can be calculated as 133° instead of the value of 110° for the homogeneous arrays. Thus, the dual hole array surface exhibits stable superhydrophobic characteristics both theoretically (159°) and experimentally (157.3°) as shown in Table 1. It should be noted that because photoresist was used for both the small and large hole patterns while bifunctional urethane methacrylate—which has lower surface energy—was used for the dual hole pattern, differences exist between the theoretical and experimental WCAs for both the small and large hole patterns.

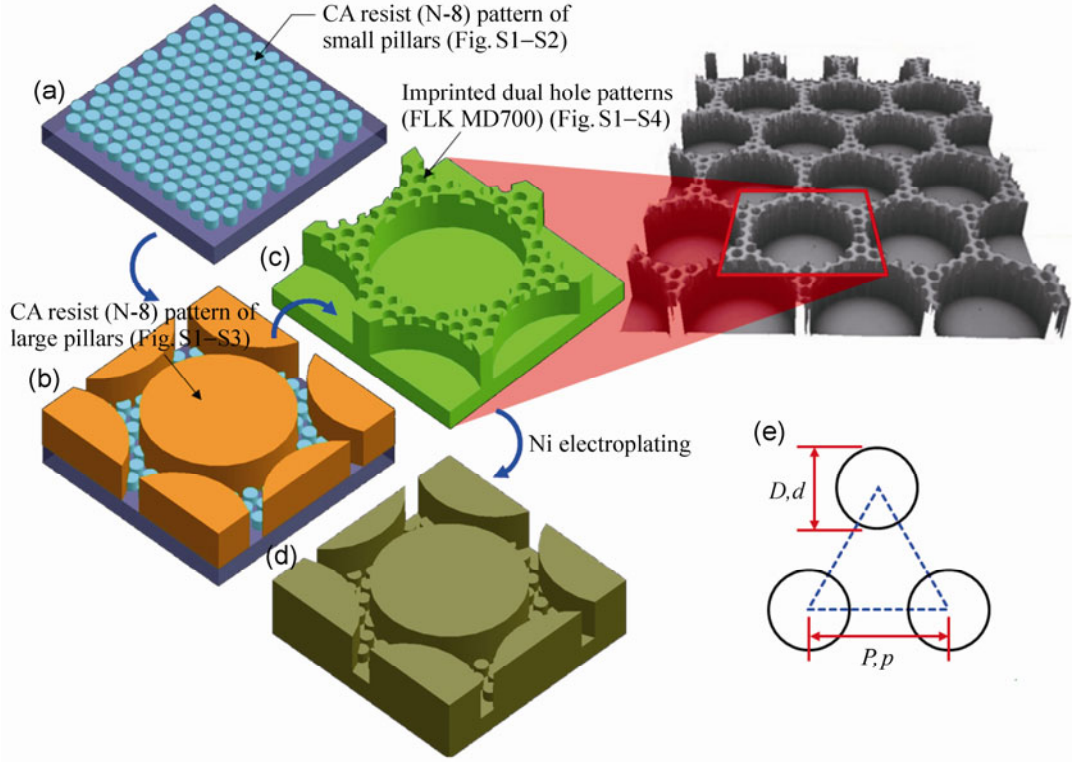

Figure 1 Schematic illustration of the preparation of a nickel stamp for superhydrophobic dual hole patterning on the CNT composite: (a) Small-sized pillar patterning (Fig. S1–S2), (b) large-sized pillar patterning (Fig. S1–S3), (c) soft stamping from dual-sized photo-resist patterns (Fig. S1–S4), (d) hard stamp fabrication by nickel electroplating, and (e) design parameters of the hexagonal arrays.

Table 1 Design parameters and theoretical contact angles for hexagonal closely packed circular hole surfaces

Design parameters		Small hole [a]	Large hole [b]	Dual hole [c]
p (μm)		8	60	60
d (μm)		6	56	56
h (μm)		7.5	20	20
θ_0 (°)		110	110	133
λ		0.75	0.93	0.93
r		2.80	1.80	1.80
ϕ_S		0.49	0.21	0.21
θ_c (°)		103	120	120
θ^*(°)	Theoretical	133.0	150.0	159.0
	Experimental	115.1	127.3	157.3
				

Further investigations into how implementation choices affect performance are currently in progress.

Using a dual hole design to obtain a superhydrophobic surface has several advantages over similarly performing pillar patterns. Importantly it avoids the fabrication complications and durability issues caused by the high aspect ratio of pillars, which easily collapse under contact. Based on the above mentioned design considerations and durability advantages, the dual hole pattern was selected for the patterning of CNT composite surfaces. Using a nickel stamp with an inverse dual hole design, a stable superhydrophobic low surface energy pattern was applied to the CNT composites.

A conventional photolithography process was utilized to prepare a nickel stamp to imprint the superhydrophobic pattern on the CNT composite as shown in Fig. 1. The nickel stamp (d) has a dual pillar pattern, which consists of small and large-sized hexagonal arrays. A cationic polymerization resin having a good patterning property was used for master pattern fabrication. The main component of this resist is an epoxy resin which cannot react with the acrylate-based resin for imprinting process. Therefore, demolding will be easy. Another important consideration for easy demolding is to increase the adhesion property between the master pattern of the dual pillar and the substrate. For this purpose, we first apply the adhesion promoter (CP-01, in-house material) to the substrate as shown in Fig. S1-1 in the Electronic Supplementary Material (ESM). Next, the small-sized pillar patterns were fabricated on the substrate on which the adhesion promoter was coated (Fig. S1-2 in the ESM) as shown in Fig. 1(a) and then the large-sized pillar patterns were constructed on top of them (Fig. S1-3 in the ESM) (b). The first step was to construct a soft polymer stamp containing the dual pillar pattern via imprinting (Fig. S1-4 in the ESM) (c). To make the soft stamp, we used bi-functional urethane methacrylate (FLK MD700, Solvay Solexsis) with 5% *w*/*w* photoinitiator (Irgacure 184, BASF) as the polymer resin. Since the perfluorinated functional blocks, which have low critical surface energy, do not participate in the polymerization, they can be exposed to the surface of the soft stamp. The soft stamp was easily separated without any pattern deformation from the photoresist dual pillar patterns. The resulting soft polymer structure is not robust enough for thermal imprinting on the CNT composite. For this application a hard material stamp with high thermal and mechanical strength must be fabricated. A hard nickel stamp (d) was successfully obtained using a nickel electroplating process to coat the fabricated polymer stamp.

3.2 Highly conducting dual hole patterned CNT composite

To achieve a highly conducting composite, the intrinsic poor conductivity of polymers can be compensated through the use of conducting filler materials which form a conducting network. Though CNTs are an ideal filler due to their unique structure and properties, achieving uniform dispersion is nontrivial as the high aspect ratio CNTs exist in heavy bundle form (up to 15 μm in diameter). Each CNT within a bundle is attached by van der Waals interactions as shown Fig. 2(a). To maximize composite performance for a given CNT wt.%, the nanotubes must be separated and then evenly dispersed within the polymer matrix. This was achieved using premixing and three-roll milling techniques, the results of which are shown in Fig. 2(b) where the results for 10 wt.% CNTs are depicted. Three-roll milling is a mixing technique that has been used to disperse highly entangled CNTs into

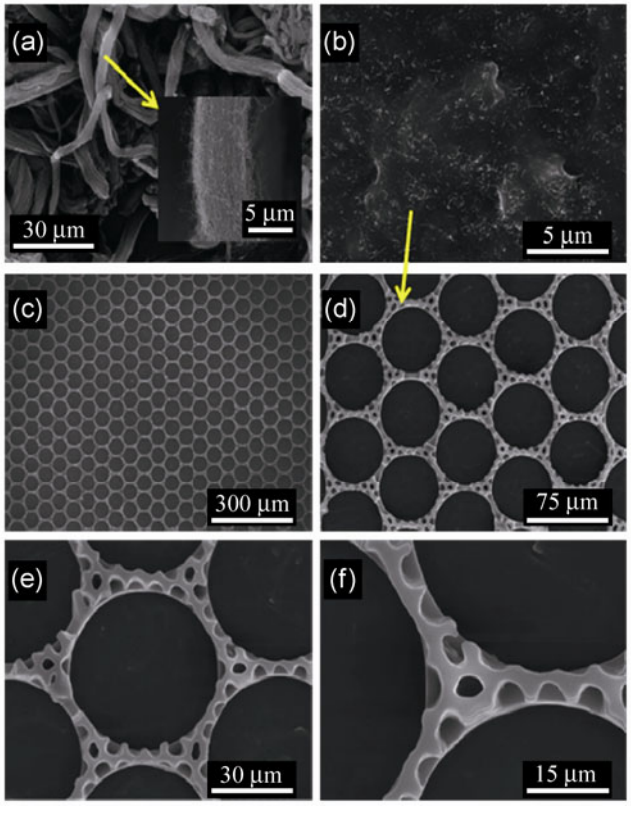

Figure 2 SEM characterization of (a) highly entangled raw CNT bundles, (b) fracture image of CNT composite (10 wt.%) with uniform dispersion conditions, (c) top-view of the surface of a dual hole patterned CNT composite (10 wt.%): Wide view (d) low resolution, (e) mid resolution, and (f) high resolution.

a polymer matrix (Fig. S2 in the ESM). During three-roll milling, shear forces created by three horizontally positioned rolls rotating in opposite directions and at different speeds disentangle the heavily bundled CNTs. The method gives a uniform shear over the entire volume of the material and results in a solvent-free, scalable process which can be used for low or high nanotube loading percentages. In addition, depending on shear intensity and time, the length of the CNTs can be shortened [25].

Using high aspect ratio nanotubes and an effective mixing process, superior conducting CNT/PDMS pastes were made where 1 wt.% filler resulted in an electrical conductivity of 1.5 S/m, and up to 301 S/m was obtained for 10 wt.% (Fig. S2 in the ESM). To integrate durable superhydrophobic surfaces with highly conducting material properties, uncured CNT/PDMS pastes were put on a hot substrate and dual pillar patterned Ni stamps were imprinted with a heat-press. After a 30-min heat impression time for curing, dual hole patterns were successfully transferred to the CNT/PDMS composites surface as clearly shown in Figs. 2(c)–2(f). The imprint techniques demonstrate the feasibility of large area impressions which could be practically expanded using roll-to-roll techniques. The high-resolution images of Figs. 2(e) and 2(f), show that the small-sized and large-sized pillars of the Ni stamp were smoothly released from the CNT paste resulting in a clean dual hole pattern. Also note that, the image in Fig. 2(b) corresponds to a cross-sectional fracture of the composite shown in Fig. 2(d), as indicated by the yellow arrow.

3.3 Surface properties with durability

As shown in Figs. 3(a) and 3(b), a water droplet on the surface of the fabricated composite (1 wt.% and 10 wt.%) has a high WCA of around 166°. This indicates that the CNT content of the composite has no noticeable influence on the effectiveness of the patterning. In fact the water repellency of the sample was so remarkable that it was impossible to measure the WCA if the volume of the water droplet at all exceeded the value normally used in conventional measurements. CAH and sliding angle is another important criterion for superhydrophobic surfaces. As shown in Fig. 3(c), when the substrate was slightly tilted (7°) the CAH of the 10 wt.% composite reached 1.5° without the droplet rolling off. But when the substrate was tilted by more than 7.5° (see Fig. 3(d)), the water droplet rolled off the substrate rapidly and left the surface completely dry. The CAH of this superhydrophobic surface is measured as 3.7° (CAH = $a - r$) where CAH < 10° indicating a self-cleaning surface. To evaluate wear durability, a column-like rubber tip under applied normal loads of 1.5 N was moved horizontally on dual patterned surface and pillar type surfaces. (Fig. S3 in the ESM). As shown in Fig. 4, even though both patterns are made from the same materials, surface durability is quite different depending on surface morphology. Pillar patterns having a high slenderness ratio are severely damaged after 100 cycles causing degradation of hydrophobicity as shown in the inset images of Fig. 4. The dual hole pattern, on the other hand, maintain its morphology and hydrophobicity after 600 cycles proving its robustness against physical damage.

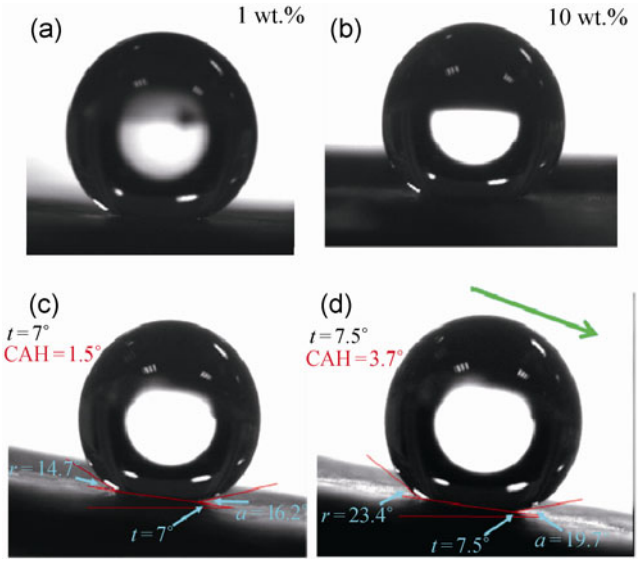

Figure 3 Photographic images of a water droplet (7 μL) on the dual hole patterned CNT composites with a contact angle of (a) 166° (1 wt.%) and (b) 167° (10 wt.%). (c) A tilted (7°) composite (10 wt.%), where the contact angle hysteresis is 1.5° without rolling off and (d) the water droplet rolled off when the composite was tilted by more than 7.5° (CAH = $a-r$ = 3.7°).

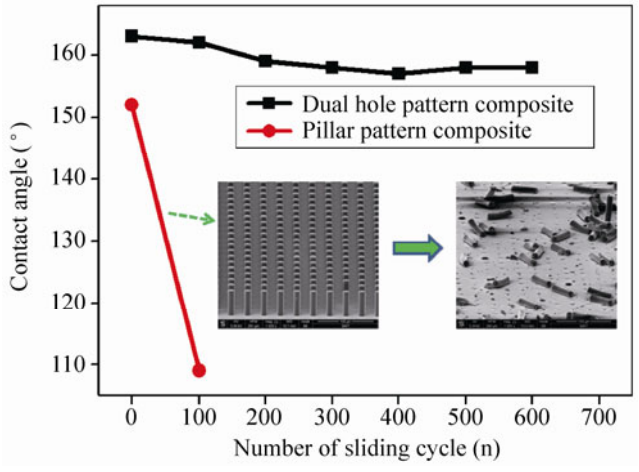

Figure 4 Contact angle of dual patterned and pillar type patterned composite films after wear tests. Rubber tip under applied normal loads of 1.5 N moved horizontally. For the pillar type case, due to the high slenderness ratio, patterns are severely damaged after 100 cycles, as shown in the inset image, causing degradation of hydrophobicity. In contrast, the dual pattern maintains its contact angle and morphology after 600 cycles showing effective durability against physical damage.

3.4 Anti-icing and deicing applications

Dual hole patterned CNT composites can be used in deicing (removal of frost) and anti-icing applications as a hybrid heater. In general, composites which exhibit high conductivity and low heat capacity are ideal for practical heating elements. In the case of CNT/PDMS composites, electrical energy can be converted into heat energy easily and quantitatively through Ohmic Joule heating. The electric heating behavior of the patterned composites was evaluated by measuring changes in resistance and temperature under an applied direct current (DC) voltage of 7 V. As shown in Fig. 5 for the 10 wt.% sample, when a voltage is applied to the composite, the normalized resistance decreases, while the temperature increases over time. After 60 s, the change in resistance saturates. It is observed that the resistances of the nanotube composites exhibit a negative temperature coefficient (NTC) behavior. This is different from pure metallic carbon nanotubes which have a positive temperature coefficient (PTC) [26]. The reason for this difference is that in the composite system, which consists of both insulating regions (polymer matrix) and conducting regions (CNTs), tube–tube interconnection resistance dominates over the metallic filler properties resulting in a NTC behavior [27, 28]. By increasing the conductivity of the composites (increased wt.%), changes in resistance during heating can be reduced while the saturated temperature attains a higher magnitude (Fig. S4 in the ESM). It should also be noted that the temperature response time, the time to reach steady-state, could be shortened by increasing the applied

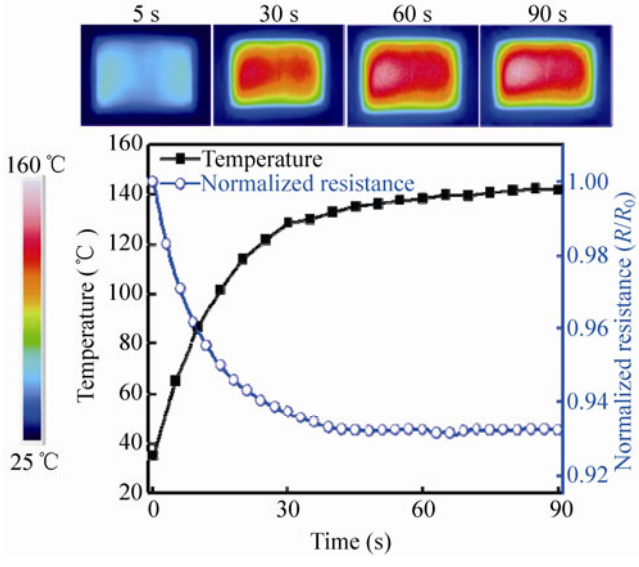

Figure 5 The electrical heating behavior of dual hole patterned CNT/PDMS composite (10 wt.%) measured as change in resistance and temperature under an applied DC voltage of 7 V.

voltage. When a previously reported conducting superhydrophobic coating created though a press and infiltration method was used as a heating element, hydrophobicity degraded due to the deformation of surface morphology during temperature increase [27]. However, the shape of the dual hole pattern on the composite used in this work is robust up to 200 ℃. In Fig. S5 (in the ESM), SEM characterization of a dual hole patterned CNT composite (10 wt.%) at different temperatures (a) room temperature, (b) 100°, (c) 180°, and (d) comparison with high resolution is shown, indicating that hydrophobicity is constant with varying temperature. After temperature cycles, the measured WCA was the same as that before heating. In addition, we have seen that the growth of ice on the dual patterned film was much lower than on a bare Al substrate at –30 ℃ (Fig. S6 in the ESM) which is consistent with our previous report [9]. Consequently, the attributes of the superhydrophobic patterned CNT composites created in this work make them ideal for anti-icing and deicing applications. For instance, the composites can be used on surfaces to reduce and/or remove ice and frost. Such a system would operate via two different mechanisms. First the superhydrophobic surface would suppress the formation of frost, acting as anti-icing material. Then, through electric heating, the remaining frost could be quickly and easily removed, where the quick response at low voltage—a consequence of the small thermal capacitance of the polymer and the high thermal conductivity of the CNT—makes for a highly controllable heating element.

3.5 EMI shielding applications

We next monitored the EMI shielding efficiency (SE) of the dual patterned composite in the microwave frequency range (8.2–12.4 GHz: X-band) using a two-port vector network analyzer. The X-band is used for both civil and military communications with applications as diverse as weather monitoring, vehicular detection, air traffic control and defense tracking [29]. The desired amount of conducting filler is generally dependent on the required SE = 10 log(P_i/P_t), where P_i and P_t are the magnitudes of the incident and transmitted power densities. For this work, composites with high aspect ratio CNTs were fabricated with patterned surfaces. The measured SE of the fabricated composites as well as that of a PDMS base matrix is shown in Fig. 6(a). The measured SE is one of the highest values ever reported for the given CNT loading and measurement conditions [30–32]. For example, compared to our previously reported results, which used lower aspect ratio CNTs (~880) within the composites, the SE dramatically increased from 15 dB to 60 dB and from 30 dB to 100 dB for 2 mm thick samples with loadings of 5 and 10 wt.% respectively [30]. The improvements measured for the new and patterned composites can be investigated by inspecting the various components of the total shielding effectiveness, SE(tot). SE(tot) is the sum of the contributions due to both the

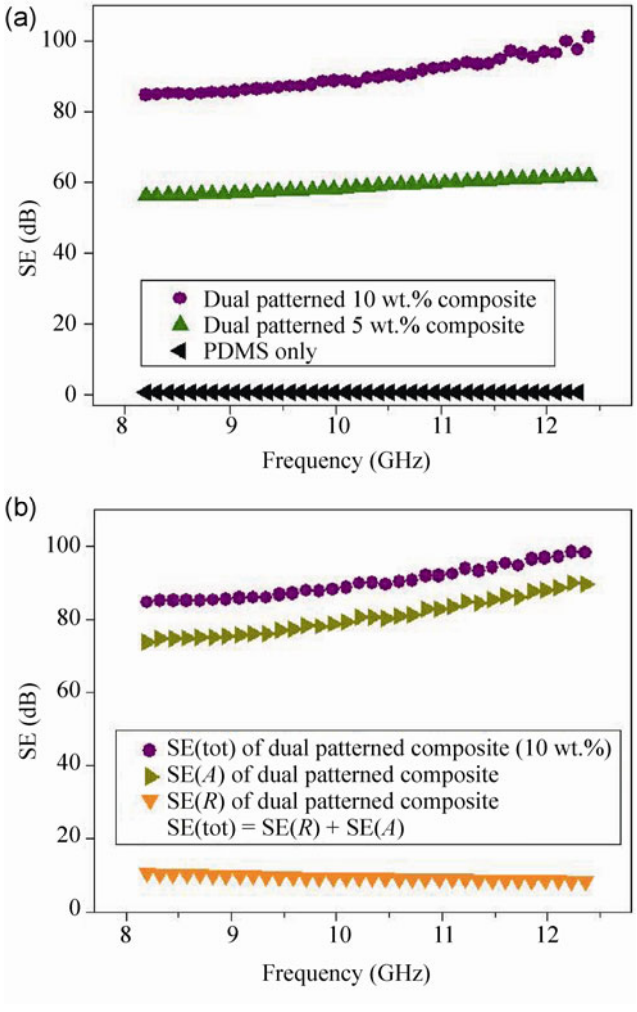

Figure 6 EMI shielding effectiveness (SE) of patterned CNT composites (5 wt.% and 10 wt.%) (a) Superior SE(tot) was found for patterned composites (thickness of 2 mm). (b) Total shielding efficiency, SE(tot), can be decomposed into contributions from reflection, SE(R) and absorption, SE(A) through a consideration of the frequency dependence (for 10 wt.%).

reflective (R) and the absorptive (A) factors, SE (tot) = SE(R) + SE(A), where SE(R) = – 10 log(1–R) and SE(A) = –10 log[T/(1–R)] [32, 33]. It was assumed that for the measured samples the affect of multiple reflections could be ignored. The R, A, and T (transmission) were then obtained through the determination of the S-parameters using a vector network analyzer, where $T = |S_{21}|^2$, $R = |S_{11}|^2$ and $A = 1 - |S_{11}|^2 - |S_{21}|^2$. In Fig. 6(b), the results indicate absorption-dominated shielding for the 10 wt.% composite, with SE(A) of the patterned composite being much higher than SE(R). In general, absorption-dominated shielding occurs in highly conducting composites [32]. The dramatic improvement likely stems from high aspect ratio of the CNTs and the increased surface area provided by the patterning. In the literature, significant differences have been reported between the absorption of a rough surface and that of a smooth surface due to the eddy currents in a conducting surface [34, 35]. Detailed investigation of the effects of aspect ratio, surface area and structure on SE(A) will be left as a topic for future research.

4 Conclusions

We have reported a new type of carbon nanotube–polymer composite which combines the bulk properties of nanocomposites with the durable superhydrophobic properties of imprinted surfaces in a single multi-functional system. The dual hole pattern was designed to avoid the use of high slenderness ratio structures resulting in a surface which is robust against physical damage. Its stable superhydrophobic properties were characterized both theoretically and experimentally. The dual patterned composites can be effectively used for anti-icing and deicing applications where their superhydrophobic surface suppresses ice formation and their quick electric heating response at low voltage eliminates remaining frost. Moreover, by incorporating high aspect ratio CNTs and increasing the conducting surface area, superior electromagnetic shielding effectiveness was attained. The measured SE is one of the highest values ever reported for the given CNT loading and measurement conditions. The above achievements are expected to lay a strong foundation for the widespread use of superhydrophobic patterned CNT composites for a whole host of applications including electromagnetic interference shielding, heating elements, solar cell electrodes and structural reinforcement.

Electronic Supplementary Material: Supplementary material (three-roll milling as a mixing technique and high electrical conductivity of CNT/PDMS composites, wear tester for durability, electric heating behavior of 7.5 and 10 wt.% CNT composites, SEM characterization of dual hole patterned CNT composite (10 wt.%) with different temperatures and anti-frost effect on dual patterned film compared with Al substrate) is available in the online version of this article at http://dx.doi.org/10.1007/ s12274-013-0316-8.

References

[1] Chung, D. D. L. Electromagnetic interference shielding effectiveness of carbon materials. *Carbon* **2001**, *39*, 279–285.

[2] Bigg, D. M.; Stutz, D. E. Plastic composites for electromagnetic interference shielding applications. *Polym. Compos.* **1983**, *4*, 40–46.

[3] Peng, M.; Liao, Z. J.; Qi, J.; Zhou, Z. Nonaligned carbon nanotubes partially embedded in polymer matrixes: A novel route to superhydrophobic conductive surfaces. *Langmuir* **2010**, *26*, 13572–13578

[4] Liu, Z. F.; Bai, G.; Huang, Y.; Li, F. F.; Ma, Y. F.; Guo, T. Y.; He, X. B.; Lin, X.; Gao, H. J.; Chen, Y. S. Microwave absorption of single-walled carbon nanotubes/soluble cross-linked polyurethane composites. *J. Phys. Chem. C* **2007**, *111*, 13696–13700.

[5] Breuer, O.; Sundararaj, U. Big returns from small fibers: A review of polymer/carbon nanotube composites. *Polym. Compos.* **2004**, *25*, 630–645.

[6] Peigney, A.; Laurent, C.; Flahaut, E.; Bacsa, R. R.; Rousset, A. Specific surface area of carbon nanotubes and bundles of carbon nanotubes. *Carbon* **2001**, *39*, 507–514.

[7] Park, S. H.; Bandaru, P. R. Improved mechanical properties of carbon nanotube/polymer composites through the use of carboxyl-epoxide functional group linkages. *Polymer* **2010**, *51*, 5071–5077.

[8] Park, S. H.; Thielemann, P.; Asbeck, P.; Bandaru, P. R. Enhanced dielectric constants and shielding effectiveness of, uniformly dispersed, functionalized carbon nanotube composites. *Appl. Phys. Lett.* **2009**, *94*, 243111.

[9] Sohn, Y.; Lee, S.; Kim, D.; Chu, K.; Kim, D.; Kim, H.; Han, I. Low temperature reliability of carbon nanotube/silicone superhydrophobic coatings. In *Proceedings of the 44th*

International Symposium on Microelectronices (IMAPS 2011), Long Beach, USA, 2011, pp 857–860.

[10] Tang, N. J.; Yang, Y.; Lin, K. J.; Zhong, W.; Au, C. T.; Du, Y. W. Synthesis of plait-like carbon nanocoils in ultrahigh yield, and their microwave absorption properties. *J. Phys. Chem. C* **2008**, *112*, 10061–10067.

[11] Neinhuis, C.; Barthlott, W. Characterization and distribution of water-repellent, self-cleaning plant surfaces. *Ann. Bot.* **1997**, *79*, 667–677.

[12] Erbil, H. Y.; Demirel, A. L.; Avci, Y.; Mert, O. Transformation of a simple plastic into a superhydrophobic surface. *Science* **2003**, *299*, 1377–1380.

[13] Nakajima, A.; Fujishima, A.; Hashimoto, K.; Watanabe, T. Preparation of transparent superhydrophobic boehmite and silica films by sublimation of aluminum acetylacetonate. *Adv. Mater.* **1999**, *11*, 1365–1368.

[14] Sun, T. L.; Tan, H.; Han, D.; Fu, Q.; Jiang, L. No platelet can adhere-largely improved blood compatibility on nanostructured superhydrophobic surfaces. *Small* **2005**, *1*, 959–963.

[15] Furstner, R.; Barthlott, W.; Neinhuis, C.; Walzel, P. Wetting and self-cleaning properties of artificial superhydrophobic surfaces. *Langmuir* **2005**, *21*, 956–961.

[16] Takei, G.; Nonogi, M.; Hibara, A.; Kitamori, T.; Kim, H. B. Tuning microchannel wettability and fabrication of multiple-step laplace valves. *Lab Chip* **2007**, *7*, 596–602.

[17] Feng, L.; Li, S. H.; Li, Y. S.; Li, H. J.; Zhang, L. J.; Zhai, J.; Song, Y. L.; Liu, B. Q.; Jiang, L.; Zhu, D. B. Super-hydrophobic surfaces: From natural to artificial. *Adv. Mater.* **2002**, *14*, 1857–1860.

[18] Krupenkin, T. N.; Taylor, J. A.; Schneider, T. M.; Yang, S. From rolling ball to complete wetting: The dynamic tuning of liquids on nanostructured surfaces. *Langmuir* **2004**, *20*, 3824–3827.

[19] Zhu, L. B.; Xiu, Y. H.; Xu, J. W.; Tamirisa, P. A.; Hess, D. W.; Wong, C. P. Superhydrophobicity on two-tier rough surfaces fabricated by controlled growth of aligned carbon nanotube arrays coated with fluorocarbon. *Langmuir* **2005**, *21*, 11208–11212.

[20] Zhang, L.; Resasco, D. E. Single-walled carbon nanotube pillars: A superhydrophobic surface. *Langmuir* **2009**, *25*, 4792–4798.

[21] Zou, J. H.; Chen, H.; Chunder, A.; Yu, Y. X.; Huo, Q.; Zhai, L. Preparation of a superhydrophobic and conductive nanocomposite coating from a carbon-nanotube-conjugated block copolymer dispersion. *Adv. Mater.* **2008**, *20*, 3337–3341.

[22] Liu, B.; He, Y. N.; Fan, Y.; Wang, X. G. Fabricating super-hydrophobic lotus-leaf-like surfaces through soft-lithographic imprinting. *Macromol. Rapid Commun.* **2006**, *27*, 1859–1864.

[23] Cassie, A. B. D.; Baxter, S. Wettability of porous surfaces. *Trans. Faraday Soc.* **1944**, *40*, 546–551

[24] Johnson, R. E.; Dettre, R. H. Contact angle hysteresis. In *Contact Angle, Wettability, and Adhesion*. Fowkes, F. M., Ed.; American Chemical Society: Washington, D. C., 1964; pp 112–135.

[25] Rosca, I. D.; Hoa, S. V. Highly conductive multiwall carbon nanotube and epoxy composites produced by three-roll milling. *Carbon* **2009**, *47*, 1958–1968.

[26] Avedisian, C. T.; Cavicchi, R. E.; McEuen, P. M.; Zhou, X. J.; Hurst, W. S.; Hodges, J. T. High temperature electrical resistance of substrate-supported single walled carbon nanotubes. *Appl. Phys. Lett.* **2008**, *93*, 252108.

[27] Hewitt, C. A.; Kaiser, A. B.; Roth, S.; Craps, M.; Czerw, R.; Carroll, D. L. Varying the concentration of single walled carbon nanotubes in thin film polymer composites, and its effect on thermoelectric power. *Appl. Phys. Lett.* **2011**, *98*, 183110.

[28] Neitzert, H. C.; Vertuccio, L.; Sorrentino, A. Epoxy/MWCNT composite as temperature sensor and electrical heating element. *IEEE Trans. Nanotechnol.* **2011**, *10*, 688–693.

[29] Pozar, D. M. *Microwave engineering*; John Wiley & Sons, Inc.: Hoboken, 1998.

[30] Huang, Y.; Li, N.; Ma, Y. F.; Du, F.; Li, F. F.; He, X. B.; Lin, X.; Gao, H. J.; Chen, Y. S. The influence of single-walled carbon nanotube structure on the electromagnetic interference shielding efficiency of its epoxy composites. *Carbon* **2007**, *45*, 1614–1621.

[31] Das, N. C.; Maiti, S. Electromagnetic interference shielding of carbon nanotube/ethylene vinyl acetate composites. *J. Mater. Sci.* **2008**, *43*, 1920–1925.

[32] Park, S. H.; Theilmann, P. T.; Asbeck, P. M.; Bandaru, P. R. Enhanced electromagnetic interference shielding through the use of functionalized carbon-nanotube-reactive polymer composites. *IEEE Trans. Nanotechnol.* **2010**, *9*, 464–469.

[33] Kim, H. M.; Kim, K.; Lee, C. Y.; Joo, J.; Cho, S. J.; Yoon, H. S.; Pejakovic, D. A.; Yoo, J. W.; Epstein, A. J. Electrical conductivity and electromagnetic interference shielding of multiwalled carbon nanotube composites containing Fe catalyst. *Appl. Phys. Lett.* **2004**, *84*, 589–591.

[34] Morgan, S. P. Effects of surface roughness on eddy current losses at microwave frequencies. *J. Appl. Phys.* **1949**, *20*, 352–362.

[35] Tsang, L.; Gli, X. X.; Braunisch, H. Effects of random rough surface on absorption by conductors at microwave frequencies. *IEEE Microw. Wirel. Compon. Lett.* **2006**, *16*, 221–223.